

This is the accepted manuscript made available via CHORUS. The article has been published as:

Universal $2\Delta_{\max}/k_B T_c$ scaling decoupled from the electronic coherence in iron-based superconductors

H. Miao, W. H. Brito, Z. P. Yin, R. D. Zhong, G. D. Gu, P. D. Johnson, M. P. M. Dean, S. Choi, G. Kotliar, W. Ku, X. C. Wang, C. Q. Jin, S.-F. Wu, T. Qian, and H. Ding

Phys. Rev. B **98**, 020502 — Published 9 July 2018

DOI: [10.1103/PhysRevB.98.020502](https://doi.org/10.1103/PhysRevB.98.020502)

Universal $2\Delta_{max}/k_B T_c$ scaling decoupled from the Electronic Coherence in Iron-Based Superconductors

H. Miao,^{1, 2,*} W. H. Brito,² Z. P. Yin,³ R. D. Zhong,² G. D. Gu,² P. D. Johnson,² M. P. M. Dean,² S. Choi,² G. Kotliar,^{2, 4} W. Ku,⁵ X. C. Wang,¹ C. Q. Jin,¹ S. -F. Wu,¹ T. Qian,¹ and H. Ding^{1, 6, †}

¹*Beijing National Laboratory for Condensed Matter Physics,
Institute of Physics, Chinese Academy of Sciences, Beijing 100190, China*

²*Condensed Matter Physics and Materials Science Department,
Brookhaven National Laboratory, Upton, New York 11973, USA*

³*Department of Physics and the Center of Advanced Quantum Studies,
Beijing Normal University, Beijing 100875, China*

⁴*Department of Physics and Astronomy, Rutgers University, Piscataway, New Jersey 08854, USA*

⁵*Physics Department, Shanghai Jiaotong University, 800 Dongchuan Road, Shanghai, 200240, China*

⁶*Collaborative Innovation Center of Quantum Matter, Beijing 100190, China*

Here we use angle-resolved photoemission spectroscopy to study superconductivity that emerges in two extreme cases, from a Fermi liquid phase (LiFeAs) and an incoherent bad-metal phase ($\text{FeTe}_{0.55}\text{Se}_{0.45}$). We find that although the electronic coherence can strongly reshape the single particle spectral function in the superconducting state, it is decoupled from the maximum-superconducting-gap and T_c ratio, $2\Delta_{max}/k_B T_c$, which shows a universal scaling that is valid for all FeSCs. Our observation excludes pairing scenarios in the BCS and the BEC limit for FeSCs and calls for a universal strong coupling pairing mechanism for the FeSCs.

The interplay between superconductivity and its normal state electronic coherence remains a central puzzle in unconventional superconductors. In the cuprate and heavy Fermion superconductors, superconductivity emerges from a non-Fermi liquid normal state with nearly vanishing coherent weight, $Z_k \rightarrow 0$, and thus motivated theoretical proposals of superconducting (SC) pairing mechanisms beyond the BCS paradigm^{1–3}. In the multi-orbital iron-based superconductors (FeSCs), the electronic structure and the total carrier density are highly sensitive to the Hund’s coupling and the height of anion atoms (As/Se) that are alternatively placed above and below the iron-plane^{4,5}. As a consequence, FeSCs display diverse phase diagrams that ignite extensive debates on the pairing mechanism mainly among BCS-like theories that utilize coherent quasi-particles (QPs) near the Fermi level^{6–8}, scenarios that emphasize localized electrons with large short-ranged antiferromagnetic (AFM) interactions^{9–13}, and strong coupling approach based on metallic continuum and spin fluctuations¹⁴. In this paper, we use angle-resolved photoemission spectroscopy (ARPES) to directly explore the evolution of the single-particle spectral function, $A(k, \omega)$, starting from two different phases: (i) a coherent Fermi-liquid phase with large carrier density in LiFeAs and (ii) an incoherent bad metal phase with small carrier density in $\text{FeTe}_{0.55}\text{Se}_{0.45}$. We find that while the change of $A(k, \omega)$ in the SC phase strongly depends on Z_k , superconductivity itself is very robust and shows a universal scaling $2\Delta_{SC}^{max}(k)/k_B T_c \sim 7.2$ for all FeSCs, where $\Delta_{SC}^{max}(k)$ is the maximum SC gap in momentum space determined by ARPES. The independence of $2\Delta_{SC}^{max}(k)/k_B T_c$ on the correlations and Z_k that vary significantly through different families, excludes pairing scenarios in the BCS and the BEC limit and calls for a unified theory for the iron-

pnicnides and chalcogenides.

In this study, we choose prototypical FeSCs, LiFeAs and $\text{FeTe}_{0.55}\text{Se}_{0.45}$, that have similar SC transition temperature. High-energy resolution ARPES data were recorded at the Institute of Physics, Chinese Academy of Sciences with a Scienta R4000 analyzer. We use the He I α ($\hbar\nu=21.2$ eV) resonance line of an helium discharge lamp. The angular and energy resolutions were set to 0.2° and 2 meV, respectively. All samples were cleaved in situ and measured in a vacuum better than 3×10^{-11} Torr. Sample orientation and the experimental geometry for the LiFeAs and $\text{FeTe}_{0.55}\text{Se}_{0.45}$ measurements are the same. Our DFT+DMFT calculations were performed at 116 K within the fully charge self-consistent combination of DFT and embedded dynamical mean field theory (DMFT)¹⁸. The DFT part of these calculations were performed with the WIEN2k package while the DMFT impurity problem was solved by using continuous time quantum Monte Carlo (CTQMC) calculations¹⁹, with a Hubbard $U = 5.0$ eV and Hund’s coupling $J = 0.8$ eV. We use experimental lattice parameters for the calculation of LiFeAs and the averaged anion height to model the $\text{FeTe}_{0.55}\text{Se}_{0.45}$ alloy²⁰.

We begin by establishing the distinct normal state electronic coherence of LiFeAs and $\text{FeTe}_{0.55}\text{Se}_{0.45}$. As shown in Fig. 1a, the pristine LiFeAs has a SC ground state and a Fermi liquid normal state with T -quadratic resistivity up to 60 K. The experimentally determined Fermi surfaces (FSs) of LiFeAs are shown in Fig. 1b: the mismatch, δ , between the large hole FS at the Γ point and the two electron FSs at the M point is found to give rise to incommensurate low-energy spin excitations^{15,21}. In $\text{FeTe}_{0.55}\text{Se}_{0.45}$, however, superconductivity is induced by suppressing the bicollinear antiferromagnetic (BC-AFM) phase (Fig. 1c). Figure 1d shows the resistivity of SC $\text{FeTe}_{0.55}\text{Se}_{0.45}$. The normal state resistivity,

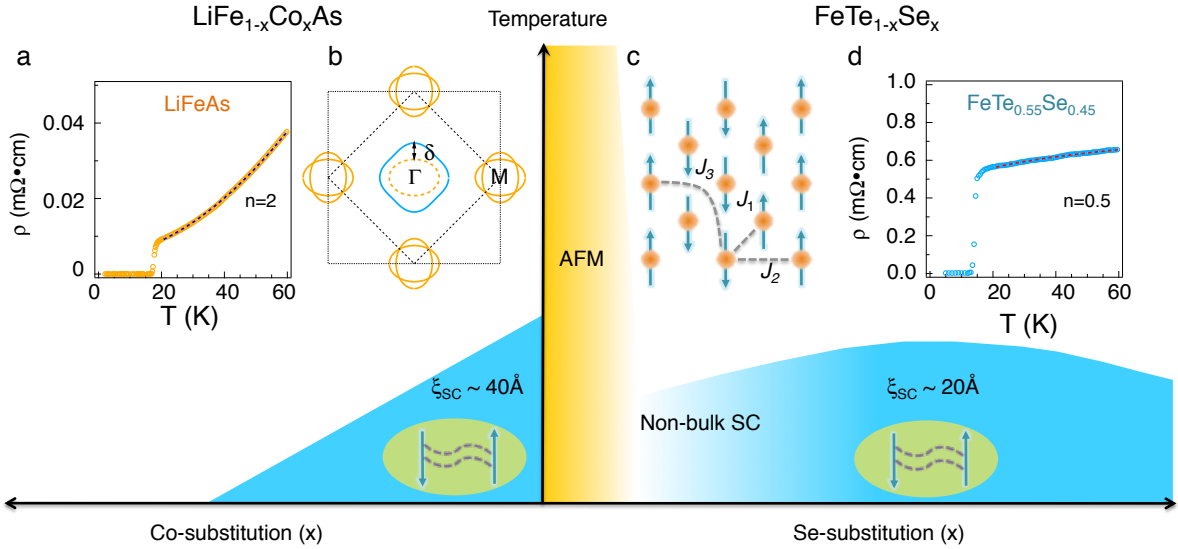


Figure 1. Schematic phase diagram of $\text{LiFe}_{1-x}\text{Co}_x\text{As}$ and $\text{FeTe}_{1-x}\text{Se}_x$. $\text{LiFe}_{1-x}\text{Co}_x\text{As}$ has simpler phase diagram, where superconductivity emerges in the pristine LiFeAs and the SC transition temperature, T_c , is linearly suppressed via electron doping. $\text{FeTe}_{1-x}\text{Se}_x$, however, has competing ground states, where superconductivity is induced by suppressing BC-AFM order and remains robust against Se substitutions. (a) Temperature dependent resistivity of LiFeAs . The dashed line is a power function, $a+bT^n$, fitting of the data. $n=2$ is found in LiFeAs demonstrating a Fermi liquid behavior up to 60 K. (b) Experimentally determined FS topology of LiFeAs . The dashed orange ellipse at the Γ point is moved from the M point to show the FS size difference, δ , that gives rise the incommensurate low-energy spin excitations¹⁵. (c) BC-AFM order of FeTe that is better described by strong coupling J_1 - J_2 - J_3 model and is not obtained by FS nesting scenario. (d) Temperature dependent resistivity of SC $\text{FeTe}_{0.55}\text{Se}_{0.45}$ shows a bad metal normal state with $n=0.5$. The superconducting coherence length, ξ_{SC} , of LiFeAs and $\text{FeTe}_{0.55}\text{Se}_{0.45}$ are 40 Å and 20 Å, respectively^{16,17}.

$\rho_{T_c}=0.56 \text{ m}\Omega \text{ cm}$, is two orders of magnitude larger than that in LiFeAs and exhibits a saturation behavior in the Mott-Ioffe-Regel limit²², with a mean free path close to the size of the unit-cell. Similar bad metal behavior has also been observed in the pristine FeTe , thus proving that the electronic incoherence is an intrinsic rather than disorder induced property^{4,20,23,24}.

The different normal state properties between LiFeAs and $\text{FeTe}_{0.55}\text{Se}_{0.45}$ are indeed captured by our DFT plus dynamic mean field theory (DFT+DMFT) calculations without spin-orbit coupling. Figures 2a and b show the DFT+DMFT calculated $A(k,\omega)$ superimposed with the ARPES determined band dispersion of LiFeAs and $\text{FeTe}_{0.55}\text{Se}_{0.45}$, respectively²⁰. As can be seen in these plots, the overall band dispersion agrees quite well with ARPES measurements without any adjustment such as band renormalization and shift. Compared with LiFeAs , the calculated spectral excitation of $\text{FeTe}_{0.55}\text{Se}_{0.45}$ is broader and more incoherent, thus reflecting its larger scattering rate and smaller Z_k . These results are in excellent agreement with ARPES measured energy distribution curves (EDCs) in the normal state ($T=20$ K) as shown in Figs. 2d and f. The resolution-limited EDCs near the Fermi level in LiFeAs directly demonstrate the existence of well defined QPs while the linewidth in $\text{FeTe}_{0.55}\text{Se}_{0.45}$ is significantly broader especially for the most correlated β band which, as we show in the light-blue-shaded area of Fig. 2f, appears as a weak shoulder on

the tail of the α' band due to the small Z_k^β . In addition, we find that due to the enhanced orbital-selective interaction in $\text{FeTe}_{0.55}\text{Se}_{0.45}$, the band width of the β band, that is mainly composed of the d_{xy} orbital character, is significantly reduced. This makes $\text{FeTe}_{0.55}\text{Se}_{0.45}$ close to a semi-metal with the total Fermi energy, E_F^{tot} , defined as the largest energy difference between the bottom of the electron bands at the M point and the top of the hole bands at the Γ point, being 25 meV to be compared with the value of 200 meV in LiFeAs ²⁰.

Having the normal state established, we now explore the corresponding $A(k,\omega)$ response in the SC state. Figures 2c and e show the same ARPES EDCs as in Figs. 2d and f but now measured in the SC phase ($T=6$ K). We find that in LiFeAs the resolution limited peaks near E_F are shifted to higher binding energies due to the formation of Bogoliubov QPs. In contrast, in $\text{FeTe}_{0.55}\text{Se}_{0.45}$, an intense and sharp coherence peak suddenly develops in the SC phase. This contrast is strongest in the shaded areas shown in Figs. 2e and f. More strikingly, the SC coherent peaks extend to momenta $k > k_F$ on the hole-like β band, indicating a non-BCS spectral function^{20,31,32}. To quantitatively compare the ARPES spectra change from the normal to SC state, we show EDCs at $k = k_F^\beta$ and $k > k_F^\beta$ of LiFeAs and $\text{FeTe}_{0.55}\text{Se}_{0.45}$ in Fig. 3. In

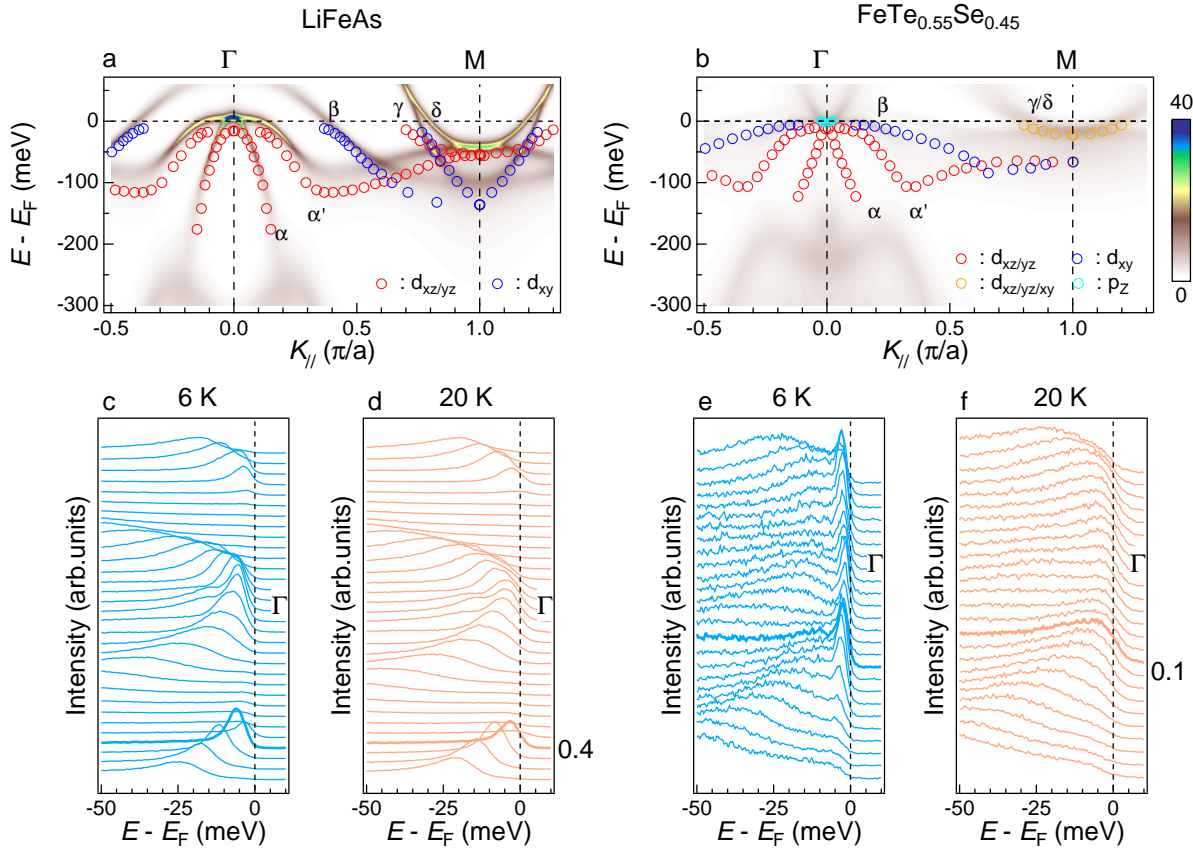


Figure 2. (a), (b) DFT+DMFT calculated $A(k,\omega)$ without spin-orbit coupling of LiFeAs and $\text{FeTe}_{0.55}\text{Se}_{0.45}$, respectively. The colorscales of (a) and (b) are the same. Colored circles are experimentally determined band dispersions along the Γ -M direction. The data point at $k_{\parallel} < 0$ is symmetrized from the data point at $k_{\parallel} > 0$. Orbital contributions of each band are showing in different colors. In the presence of spin-orbital coupling, the α' band will be pushed upward and cross E_F near the Γ point^{25,26}. We note that the shallow electron pocket at the Γ point in $\text{FeTe}_{0.55}\text{Se}_{0.45}$ is not evident in our raw data, but has been clearly observed in laser-ARPES with improved momentum resolution^{27,28}. ARPES measured EDCs below and above T_c in LiFeAs and $\text{FeTe}_{0.55}\text{Se}_{0.45}$ are shown in (c), (d) and (e), (f) respectively. The shaded area in (e) and (f) cover the d_{xy} band near E_F . The thick EDC at $0.4 \pi/a$ in LiFeAs and $0.1 \pi/a$ in $\text{FeTe}_{0.55}\text{Se}_{0.45}$ are corresponding to their k_F^{β} . Due to the intrinsic incoherence of the β band in $\text{FeTe}_{0.55}\text{Se}_{0.45}$, k_F^{β} is determined by the minimum gap position in the SC phase and consistent with previous studies^{24,27,29,30}.

the BCS theory, the SC spectral function is expressed as:

$$A(k, \omega) = \frac{1}{2} \left[\frac{\Gamma_k(1 + \frac{\xi_k}{E_k})}{(\omega - E_k)^2 + \Gamma_k^2} + \frac{\Gamma_k(1 - \frac{\xi_k}{E_k})}{(\omega + E_k)^2 + \Gamma_k^2} \right] \quad (1)$$

with

$$E_k = \sqrt{\xi_k^2 + \Delta_k^2} \quad (2)$$

where E_k and ξ_k are the EDC peak position in the SC and normal states, respectively, and Δ_k is the SC gap. In LiFeAs, the change of EDCs is largest near k_F and get smaller when $\xi_k \gg \Delta_k$, consistent with Eq. 1 and 2. In addition, we find that the total spectral weight of the symmetrized EDC at $k = k_F^{\beta}$ is nearly conserved, which, again, is in agreement with the BCS spectral function. In $\text{FeTe}_{0.55}\text{Se}_{0.45}$, however, the change of EDCs is very similar to those observed in the anti-nodal region of cuprates,

where the SC coherent peak develops from the incoherent normal state and gains more spectral weight³⁴. In Fig. 3e, we symmetrize EDCs at k_F^{β} at 6 K, 10 K, 14 K and 20 K, and then subtract the 20 K symmetrized intensity. Apparently, the SC coherent spectral weight and the total integrated spectra, I^{int} , in ± 20 meV energy window are continuously increasing as we cool to lower temperature. As shown in Fig. 3f, I^{int} indeed tracks the trend of the temperature dependent superfluid density extracted from ref.³³.

Despite the dramatic differences on $A(k, \omega)$ and normal state electronic coherence, we find that both LiFeAs and $\text{FeTe}_{0.55}\text{Se}_{0.45}$ have the same dimensionless quantity $2\Delta_{SC}^{max}(k)/k_B T_c \sim 7.2$, where Δ_{SC}^{max} is the largest SC gap determined by ARPES. This value is twice larger than that predicted by the BCS theory, confirming the strong pairing nature of these two materials. More in-

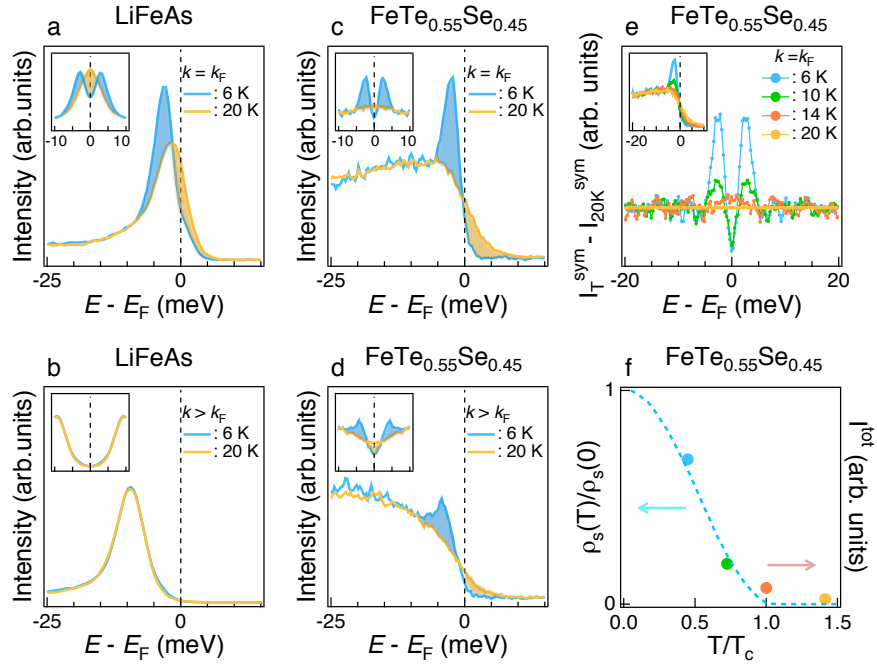


Figure 3. (a), (b) EDCs at $k = k_F^\beta$ and $k > k_F^\beta$ ($0.45\pi/a$) in LiFeAs. Inset panels show the symmetrized EDCs in (a) and (b). (c), (d) EDCs at $k = k_F^\beta$ and $k > k_F^\beta$ ($0.2\pi/a$) in $\text{FeTe}_{0.55}\text{Se}_{0.45}$ show enhanced total spectral weight in the SC phase. (e) Temperature dependent symmetrized EDCs at $k = k_F^\beta$. The 20 K data is subtracted from each symmetrized EDCs. Inset shows the temperature dependent raw data at $k = k_F^\beta$. (f) The integrated intensity of the data in (e) follows the trend of temperature dependent superfluid density in $\text{FeTe}_{1-x}\text{Se}_x$ ³³. The temperature dependent EDCs are normalized by their total counting time.

triguingly, as shown in Fig. 4, this relation is indeed ubiquitous for all FeSCs covering a wide range of electron filling and distinct FS topologies, dimensionality, impurity level, correlation strength and proximity to quantum criticality. This remarkable universality strongly indicates that all FeSCs share a universal strong coupling pairing mechanism, where the $2\Delta_{SC}^{max}(k)/k_B T_c$, at the lowest order, is decoupled from the normal state electronic coherence. The large impact of the electronic coherence in the normal state on $A(k, \omega)$ in the SC phase is therefore a consequence of the universal and robust SC pairing: the formation of coherent superconductivity, regardless of its microscopic mechanism, reduces the kinetic energy³⁵ and hence increases the coherent weight of the spectral function. This mechanism is expected to be weak in LiFeAs as the condensed electron pairs mainly originate from the coherent Fermi liquid state. We also note that in iron-pnictides, the Δ_{max} is observed on the hole bands at the Γ point with d_{xz}/d_{yz} orbital characters, while in iron-chalcogenides, the Δ_{max} is observed on the electron bands at the M point with mixed orbital characters. Finally we do not find a simple scaling relation for the minimal superconducting gap, Δ_{min} , indicating the sub-dominant role of Δ_{min} for the pairing mechanism of FeSCs.

Very recently, the BCS-BEC crossover scenario has been proposed as the possible pairing mechanism for

$\text{FeTe}_{0.55}\text{Se}_{0.45}$ ^{27,30,36}, as the SC gap near the Γ point is comparable to the E_F of the β band. As we have already shown in Fig. 2, both $\text{FeTe}_{0.55}\text{Se}_{0.45}$ and LiFeAs have shallow hole-like FSs near the Γ point, and in LiFeAs, the $E_F^{\alpha'}$ is even smaller than $\Delta^{\alpha'}$ and can in fact be negative after electron doping²⁶. However, no evidence of BCS-BEC crossover behaviors, such as the pseudogap³⁷ or deviation of BCS spectral function³⁸, have been observed. We point out that in multi-band systems, like the FeSCs, the relevant physical quantity should be E^{tot} that we defined before, rather than the E_F for an individual band. Indeed, using the experimentally determined values of $\Delta_{max}=4.2$ meV^{20,29} and $E^{tot}=25$ meV, we can nicely reproduce the recently observed Caroli-de Gennes-Martricon states in $\text{FeTe}_{0.55}\text{Se}_{0.45}$ ³⁶. Furthermore, the BCS-BEC crossover scenario is not compatible with the observed universal pairing amplitude with 10 times different E^{tot} in LiFeAs and $\text{FeTe}_{0.55}\text{Se}_{0.45}$, and hence cannot be a key ingredient of SC pairing mechanism in FeSCs.

Finally we compare our observations with the cuprate superconductors. While the origin of the electronic interactions and consequently the nature of the normal states are different between the cuprates and FeSCs, their SC response in the charge and spin excitations are remarkably similar. Spin resonance, Ω_{res} , has been observed in both high- T_c families^{39–41}. The quantity $\Omega_{res}/k_B T_c \sim 5.3$ in the cuprates³⁹ is larger than $\Omega_{res}/k_B T_c \sim 4.4$ in

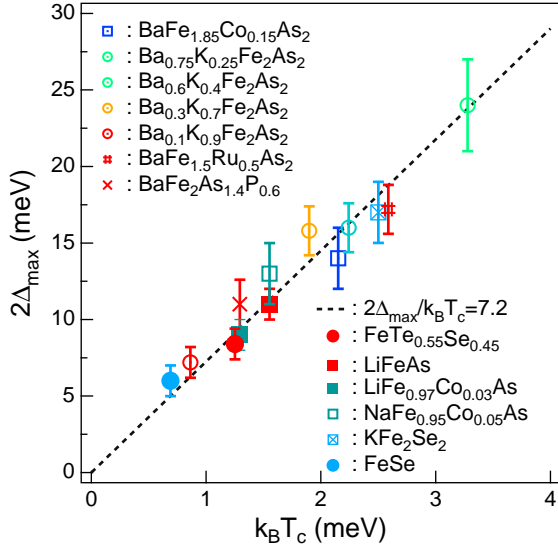


Figure 4. Summary of $2\Delta_{SC}^{max}/k_B T_c$ in various FeSCs that are determined by ARPES^{29,43–52}. The dashed line is a linear function fit of the data points.

the FeSCs⁴², reflecting a globally larger superconducting energy scale in the cuprate. In addition, the shape of $A(k, \omega)$ in the SC phase is also strongly affected by

its normal state Z_k in the cuprates, where a BCS-like spectral function is observed near the nodal region and a non-BCS spectral function emerges from the anti-nodal region^{31,32}. All these similarities suggest unconventional superconductors, including the cuprates and FeSCs, may share a common thread where both the short-ranged AFM spin fluctuations and itinerant carrier are crucial for the pairing mechanism.

ACKNOWLEDGMENTS

We thank Y. Cao, Y. M. Dai, P. Richard, Y.-L. Wang and W.-G. Yin for useful discussions. H. M., R. D. Z., M.P.M.D and P.D.J. were supported by the Center for Emergent Superconductivity, an Energy Frontier Research Center funded by the U.S. DOE, Office of Basic Energy Sciences. Z.P.Y. was supported by the National Natural Science Foundation of China (Grant No. 11674030), the Fundamental Research Funds for the Central Universities (Grant No.310421113) and the National Key Research and Development Program of China through Contract No. 2016YFA0302300. G.D.G. was supported by the Office of Basic Energy Sciences (BES), U.S. Department of Energy (DOE), through Contract No. de-sc0012704.

* hmiao@bnl.gov

† dingh@iphy.ac.cn

- ¹ P. A. Lee, N. Nagaosa, and X.-G. Wen, Rev. Mod. Phys. **78**, 17 (2006).
- ² A. Garg, M. Randeria, and N. Trivedi, Nat Phys **4**, 762 (2008).
- ³ B. Keimer, S. A. Kivelson, M. R. Norman, S. Uchida, and J. Zaanen, Nature **518**, 179 (2015).
- ⁴ Z. P. Yin, K. Haule, and G. Kotliar, Phys. Rev. B **86**, 195141 (2012).
- ⁵ N. Kurita, K. Kitagawa, K. Matsubayashi, A. Kismarahaardja, E.-S. Choi, J. S. Brooks, Y. Uwatoko, S. Uji, and T. Terashima, Journal of the Physical Society of Japan **80**, 013706 (2011).
- ⁶ I. I. Mazin, D. J. Singh, M. D. Johannes, and M. H. Du, Phys. Rev. Lett. **101**, 057003 (2008).
- ⁷ K. Kuroki, S. Onari, R. Arita, H. Usui, Y. Tanaka, H. Kontani, and H. Aoki, Phys. Rev. Lett. **101**, 087004 (2008).
- ⁸ H. Kontani and S. Onari, Phys. Rev. Lett. **104**, 157001 (2010).
- ⁹ K. Seo, B. A. Bernevig, and J. Hu, Phys. Rev. Lett. **101**, 206404 (2008).
- ¹⁰ Q. Si and E. Abrahams, Phys. Rev. Lett. **101**, 076401 (2008).
- ¹¹ T. Yildirim, Phys. Rev. Lett. **101**, 057010 (2008).
- ¹² J. Hu and H. Ding, Scientific Reports **2**, 381 (2012).
- ¹³ J. C. S. Davis and D.-H. Lee, Proceedings of the National Academy of Sciences **110**, 17623 (2013), <http://www.pnas.org/content/110/44/17623.full.pdf>.
- ¹⁴ Z. P. Yin, K. Haule, and G. Kotliar, Nat Phys **10**, 845

(2014).

- ¹⁵ M. Wang, M. Wang, H. Miao, S. V. Carr, D. L. Abernathy, M. B. Stone, X. C. Wang, L. Xing, C. Q. Jin, X. Zhang, J. Hu, T. Xiang, H. Ding, and P. Dai, Phys. Rev. B **86**, 144511 (2012).
- ¹⁶ M. P. Allan, A. W. Rost, A. P. Mackenzie, Y. Xie, J. C. Davis, K. Kihou, C. H. Lee, A. Iyo, H. Eisaki, and T.-M. Chuang, Science **336**, 563 (2012).
- ¹⁷ J.-X. Yin, Z. Wu, J.-H. Wang, Z.-Y. Ye, J. Gong, X.-Y. Hou, L. Shan, A. Li, X.-J. Liang, X.-X. Wu, J. Li, C.-S. Ting, Z.-Q. Wang, J.-P. Hu, P.-H. Hor, H. Ding, and S. H. Pan, Nat Phys **11**, 543 (2015).
- ¹⁸ K. Haule, C.-H. Yee, and K. Kim, Phys. Rev. B **81**, 195107 (2010).
- ¹⁹ K. Haule, Phys. Rev. B **75**, 155113 (2007).
- ²⁰ See Supplemental Material at [URL will be inserted by publisher] for Sample preparation/Band dispersion/Fermi Energy in FeSCs/The BCS spectral function/The Superconducting gap on different band/Universal Scaling/DFT+DMFT calculation.
- ²¹ J. Knolle, V. B. Zabolotnyy, I. Eremin, S. V. Borisenko, N. Qureshi, M. Braden, D. V. Evtushinsky, T. K. Kim, A. A. Kordyuk, S. Sykora, C. Hess, I. V. Morozov, S. Wurmehl, R. Moessner, and B. Büchner, Phys. Rev. B **86**, 174519 (2012).
- ²² C. C. Homes, A. Akrap, J. S. Wen, Z. J. Xu, Z. W. Lin, Q. Li, and G. D. Gu, Phys. Rev. B **81**, 180508 (2010).
- ²³ Y. M. Dai, A. Akrap, J. Schneeloch, R. D. Zhong, T. S. Liu, G. D. Gu, Q. Li, and C. C. Homes, Phys. Rev. B **90**, 121114 (2014).

- ²⁴ E. Ieki, K. Nakayama, Y. Miyata, T. Sato, H. Miao, N. Xu, X.-P. Wang, P. Zhang, T. Qian, P. Richard, Z.-J. Xu, J. S. Wen, G. D. Gu, H. Q. Luo, H.-H. Wen, H. Ding, and T. Takahashi, Phys. Rev. B **89**, 140506 (2014).
- ²⁵ P. D. Johnson, H.-B. Yang, J. D. Rameau, G. D. Gu, Z.-H. Pan, T. Valla, M. Weinert, and A. V. Fedorov, Phys. Rev. Lett. **114**, 167001 (2015).
- ²⁶ H. Miao, T. Qian, X. Shi, P. Richard, T. K. Kim, M. Hoesch, L. Y. Xing, X.-C. Wang, C.-Q. Jin, J.-P. Hu, and H. Ding, Nat Commun **6** (2015).
- ²⁷ K. Okazaki, Y. Ito, Y. Ota, Y. Kotani, T. Shimojima, T. Kiss, S. Watanabe, C.-T. Chen, S. Niitaka, T. Hanaguri, H. Takagi, A. Chainami, and S. Shin, Scientific Reports **4**, 4109 (2014).
- ²⁸ P. Zhang, K. Yaji, T. Hashimoto, Y. Ota, T. Kondo, K. Okazaki, Z. Wang, J. Wen, G. D. Gu, H. Ding, and S. Shin, Science **360**, 182 (2018).
- ²⁹ H. Miao, P. Richard, Y. Tanaka, K. Nakayama, T. Qian, K. Umezawa, T. Sato, Y.-M. Xu, Y. B. Shi, N. Xu, X.-P. Wang, P. Zhang, H.-B. Yang, Z.-J. Xu, J. S. Wen, G.-D. Gu, X. Dai, J.-P. Hu, T. Takahashi, and H. Ding, Phys. Rev. B **85**, 094506 (2012).
- ³⁰ S. Rinott, K. B. Chashka, A. Ribak, E. D. L. Rienks, A. Taleb-Ibrahimi, P. Le Fevre, F. Bertran, M. Randeria, and A. Kanigel, Science Advances **3** (2017), 10.1126/sciadv.1602372.
- ³¹ D. L. Feng, D. H. Lu, K. M. Shen, C. Kim, H. Eisaki, A. Damascelli, R. Yoshizaki, J.-i. Shimoyama, K. Kishio, G. D. Gu, S. Oh, A. Andrus, J. O'Donnell, J. N. Eckstein, and Z.-X. Shen, Science **289**, 277 (2000).
- ³² H. Ding, J. R. Engelbrecht, Z. Wang, J. C. Campuzano, S.-C. Wang, H.-B. Yang, R. Rogan, T. Takahashi, K. Kadouwaki, and D. G. Hinks, Phys. Rev. Lett. **87**, 227001 (2001).
- ³³ H. Kim, C. Martin, R. T. Gordon, M. A. Tanatar, J. Hu, B. Qian, Z. Q. Mao, R. Hu, C. Petrovic, N. Salovich, R. Giannetta, and R. Prozorov, Phys. Rev. B **81**, 180503 (2010).
- ³⁴ A. V. Fedorov, T. Valla, P. D. Johnson, Q. Li, G. D. Gu, and N. Koshizuka, Phys. Rev. Lett. **82**, 2179 (1999).
- ³⁵ J. E. Hirsch, Science **295**, 2226 (2002).
- ³⁶ M. Chen, X. Chen, H. Yang, Z. Du, X. Zhu, E. Wang, and H.-H. Wen, Nature Communications **9**, 970 (2018).
- ³⁷ M. Randeria and E. Taylor, Annual Review of Condensed Matter Physics **5**, 209 (2014), <https://doi.org/10.1146/annurev-conmatphys-031113-133829>.
- ³⁸ Y. Lubashevsky, E. Lahoud, K. Chashka, D. Podolsky, and A. Kanigel, Nat Phys **8**, 309 (2012).
- ³⁹ M. Eschrig, Advances in Physics **55**, 47 (2006).
- ⁴⁰ P. Dai, Rev. Mod. Phys. **87**, 855 (2015).
- ⁴¹ Q. Wang, Y. Shen, B. Pan, X. Zhang, K. Ikeuchi, K. Iida, A. D. Christianson, H. C. Walker, D. T. Adroja, M. Abdel-Hafiez, X. Chen, D. A. Chareev, A. N. Vasiliev, and J. Zhao, Nature Communications **7**, 12182 (2016).
- ⁴² Z. Wang, H. Yang, D. Fang, B. Shen, Q.-H. Wang, L. Shan, C. Zhang, P. Dai, and H.-H. Wen, Nature Physics **9**, 42 (2012).
- ⁴³ K. Terashima, Y. Sekiba, J. H. Bowen, K. Nakayama, T. Kawahara, T. Sato, P. Richard, Y.-M. Xu, L. J. Li, G. H. Cao, Z.-A. Xu, H. Ding, and T. Takahashi, Proceedings of the National Academy of Sciences **106**, 7330 (2009).
- ⁴⁴ K. Nakayama, T. Sato, P. Richard, Y.-M. Xu, T. Kawahara, K. Umezawa, T. Qian, M. Neupane, G. F. Chen, H. Ding, and T. Takahashi, Phys. Rev. B **83**, 020501 (2011).
- ⁴⁵ X.-P. Wang, T. Qian, P. Richard, P. Zhang, J. Dong, H.-D. Wang, C.-H. Dong, M.-H. Fang, and H. Ding, EPL (Europhysics Letters) **93**, 57001 (2011).
- ⁴⁶ N. Xu, P. Richard, X.-P. Wang, X. Shi, A. van Roekeghem, T. Qian, E. Ieki, K. Nakayama, T. Sato, E. Rienks, S. Thirupathaiah, J. Xing, H.-H. Wen, M. Shi, T. Takahashi, and H. Ding, Phys. Rev. B **87**, 094513 (2013).
- ⁴⁷ Z.-H. Liu, P. Richard, K. Nakayama, G.-F. Chen, S. Dong, J.-B. He, D.-M. Wang, T.-L. Xia, K. Umezawa, T. Kawahara, S. Souma, T. Sato, T. Takahashi, T. Qian, Y. Huang, N. Xu, Y. Shi, H. Ding, and S.-C. Wang, Phys. Rev. B **84**, 064519 (2011).
- ⁴⁸ H. Miao, Z. P. Yin, S. F. Wu, J. M. Li, J. Ma, B.-Q. Lv, X. P. Wang, T. Qian, P. Richard, L.-Y. Xing, X.-C. Wang, C. Q. Jin, K. Haule, G. Kotliar, and H. Ding, Phys. Rev. B **94**, 201109 (2016).
- ⁴⁹ H. Ding, P. Richard, K. Nakayama, K. Sugawara, T. Arakane, Y. Sekiba, A. Takayama, S. Souma, T. Sato, T. Takahashi, Z. Wang, X. Dai, Z. Fang, G. F. Chen, J. L. Luo, and N. L. Wang, EPL (Europhysics Letters) **83**, 47001 (2008).
- ⁵⁰ N. Xu, P. Richard, X. Shi, A. van Roekeghem, T. Qian, E. Razzoli, E. Rienks, G.-F. Chen, E. Ieki, K. Nakayama, T. Sato, T. Takahashi, M. Shi, and H. Ding, Phys. Rev. B **88**, 220508 (2013).
- ⁵¹ Y. Zhang, Z. R. Ye, Q. Q. Ge, F. Chen, J. Jiang, M. Xu, B. P. Xie, and D. L. Feng, Nature Physics **8**, 371 (2012).
- ⁵² D. Liu, C. Li, J. Huang, B. Lei, L. Wang, X. Wu, B. Shen, Q. Gao, Y. Zhang, X. Liu, Y. Hu, Y. Xu, A. Liang, J. Liu, P. Ai, L. Zhao, S. He, L. Yu, G. Liu, Y. Mao, X. Dong, X. Jia, F. Zhang, S. Zhang, F. Yang, Z. Wang, Q. Peng, Y. Shi, J. Hu, T. Xiang, X. Chen, Z. Xu, C. Chen, and X. J. Zhou, **2**, 1 (2018), arXiv:1802.02940v1.